Energy Proceedings
Vol 30, 2023
ISSN 2004-2965

Comprehensive Analysis for the Impact of Hydrogen Blending on the Economic and Environmental Performance of Natural Gas Pipeline Network

Bo Zhang [1], Ning Xu [1*], Haoran Zhang [2], Bohong Wang [3], Rui Qiu[1], Qi Liao [1], Yongtu Liang [1*]

1 China University of Petroleum-Beijing, Fuxue Road No. 18, Changping District, Beijing, 102249, China

2 Center for Spatial Information Science, The University of Tokyo, 5-1-5 Kashiwanoha, Kashiwa, Chiba, 277-8563, Japan

3 Zhejiang Ocean University, No. 1 Haida South Road, Zhoushan, 316022, China

ABSTRACT

Blending hydrogen into the existing natural gas pipeline network is regarded as a potential mode in the future. However, the influence of hydrogen on the economic and environmental performance of natural gas pipeline networks remained unclear. This paper established a mathematical programming model to get the optimal operation plan of the pipeline system under different hydrogen blending ratios, and the operation costs and carbon emissions of the hydrogen mixed system are analyzed accordingly. The studied case demonstrated that: (1) The optimization model has significant potential in reducing the economic cost and carbon emission of the system with an average decrease of 11.48%. (2) For every 1% of hydrogen added, the annual operating cost varies from minus $0.73 million to positive $1.67 million, and carbon emission varies from minus 0.38 kiloton to $0.76 kiloton. The proposed optimization model can provide theoretical guidance for the further application of this transportation mode.

Keywords: Natural gas pipeline, Hydrogen blending, 2-E analysis, Optimization

1. INTRODUCTION

Under the background of the rapid development of hydrogen energy, more research is paid to the hydrogen industry chain and hydrogen transportation mode[1]. Hydrogen can be transported using several modes like pure hydrogen pipeline in the gaseous state, tanker truck in the liquid state, adsorption & desorption in the solid state, and blending into natural gas pipeline [2], etc. Among them, blending hydrogen into the existing natural gas pipeline is expected to become an effective way for utility-scale and long-distance applications because this method can avoid the cost of constructing large-scale pure hydrogen pipelines or other expensive infrastructure [3].

Since the density, calorific value, compressibility, and other physical parameters of the mixed gas after hydrogen blending differ greatly from the original pure natural gas, it will inevitably cause changes in the economic and environmental conditions of the natural gas pipeline system.

Problems that occurred in pipeline transportation after hydrogen blending can be divided into four categories, namely, the compatibility of pipeline material with hydrogen, the adaptability of the transportation process to hydrogen, the influence of hydrogen on the pipeline integrity, and the gas interchangeability of hydrogen and natural gas [4]. Among them, this paper is focused on the adaptability of the transportation process to hydrogen, which mainly considers the changes in the density, calorific value, compressibility, and other properties of the mixed gas after hydrogen doping. Then, uses the gas flow theory to explore the variation of operating parameters of the pipeline, compressor, turbine, and other equipment with the hydrogen doping ratio.

Existing researches about the influence of hydrogen on the operation parameters of natural gas pipeline network have two main deficiencies. Firstly, the operating plan of the compressor remains unchanged when hydrogen is added to the pipeline, otherwise, the operating scheme is not been optimized or adjusted according to the physical property of the mixed gas. Secondly, the influence of hydrogen on the operation parameters of pipeline system is analyzed based on the fixed offload boundary condition.

For the first point, previous studies mainly considered certain states of the compressor. For instance, the compressor is controlled at a fixed rotational speed or a fixed outlet pressure. When hydrogen is dropped into the pipeline, the compressor maintains the fixed control value without adjustment. However, the operation parameters of the compressor may change greatly along with the hydrogen blending ratio due to the change in

the physical properties of mixed gas. The former operation state of the compressor is not effectively applied to the mixed gas. Consequently, it is necessary to determine the new operation state or the controlled value of the compressor. For the second point, most conclusions of recent studies are based on the constant control mode of the offload station. Specifically, the end of the pipeline (offload stations) or the outer boundary can be controlled by different modes. Compared with the scenario without hydrogen doping, users can keep the offload pressure unchanged after hydrogen doping. Similarly, the flow rate or the heat flow rate can also remain unchanged. Based on the fact that different control modes will cause the distinct operating condition, the promoted study of operating parameters after hydrogen blending by considering all-around control modes is needed.

In summary, a new operation plan for the compressor under different hydrogen blending ratios is needed. Since the energy consumption (hydraulic) optimization of the compressor has significant potential in improving the operating efficiency and reducing the operating cost, this paper used the aforementioned method to get the optimal plan. Besides, the influence of hydrogen on the operation parameters of the pipeline system under different boundary conditions shall be analyzed. So, this paper proceeded with the research by different scenario settings to represent real boundaries.

Therefore, this paper proposed an economic optimization model to reduce the energy consumption of the compressors when hydrogen is blended in the pipeline system. The model includes the continuity constraint, flow constraint, equation of state constraint and detailed characteristic curve constraint of the compressor, etc. Besides, this paper proposed four scenarios to represent different boundary conditions, namely, the baseline scenario (BS), the setpoint of flow rate scenario (SF), the setpoint of pressure scenario (SP), and the setpoint of heat flow rate scenario (SH). Then, the optimal operation parameters for different hydrogen blending ratios are determined and the variation of the economic and environmental conditions with the hydrogen doping ratio in different scenarios was analyzed.

2. METHODOLOGY

2.1 Objective function

The maximum hydrogen blending ratio is set as the objective function of the single source natural gas pipeline as Equ.1 shown.

$$max\ f = \theta \tag{1}$$

Where θ denotes the hydrogen blending ratio.

Concerning a certain hydrogen blending amount, an operation optimization model with the minimum energy consumption of the compressor as the objective function is established to obtain the best operating point (see Equ.2).

$$min\ g = \sum_{(i,j)\in A^C} N_{i,j} \tag{2}$$

Where, $\mathrm{N_{I,j}}$ represents the power of the compressor which is characterized by an arc from node i to node j, (kW). g is the summation of all the compressors' power and $\forall(\mathrm{I,j}) \in \mathrm{A^C}$ is the set of all the compressor arcs.

2.2 Constraints

The governing equations which give the relationship between the pressure and the flow rate in a straight pipe can be derived as follows. The governing equation applies to any pipeline ($\forall(\mathrm{I,j}) \in \mathrm{A^P}$).

$$p_i^2 - p_j^2 = \frac{\lambda Z \Delta_* T}{C_0^2 D_{i,j}^5} L_{i,j} Q_{i,j}^2, \forall (i,j) \in A^P \tag{3}$$

Where $\mathrm{p_I}$ and $\mathrm{p_j}$ indicate the pressure at the start point and endpoint of the pipeline (bar); λ is the Darcy friction factor which is a function of Reynolds number (Re) and the relative roughness of the pipeline ($\frac{\varepsilon}{\mathrm{D}}$). Z is the compressibility factor that is used to alter the ideal gas equation to account for the real gas behavior (see Equ.4). Δ_* is the ratio of gas density to dry air density. T is the temperature (K). $\mathrm{C_0}$ is the unit factor. $\mathrm{D_{I,j}}$ is the pipeline diameter (mm). $\mathrm{L_{I,j}}$ is the pipeline length (km). $\mathrm{Q_{I,j}}$ is the pipe flow rate ($\frac{m^3}{d}$).

$$Z = (\rho RT + (B_0 RT - A_0 - \frac{C_0}{T^2} + \frac{D_0}{T^3} + \frac{E_0}{T^4})\rho^2 + (bRT - a - \frac{d}{T}) + \alpha(a + \frac{d}{T})\rho^6 + \frac{c\rho^3}{T^2}(1 + \gamma\rho^2)\, exp(-\gamma\rho^2))/\rho RT \tag{4}$$

ρ is the gas density (kg/m^3), R is the universal gas constant $8.314kJ/(kmol \cdot K)$, in addition to the $\rho, \mathrm{R}, \mathrm{T}$, all the other characters such as $\mathrm{A_0}, \mathrm{B_0}$ are 11 parameters respectively.

Equations representing a network's interconnection are based on Kirchhoff's first law[4], which states that the flow into or out of a node in a network is zero because of the mass conservation. The mathematical relationship is expressed as follows and the equation applies to any nodes ($\forall \mathrm{i} \in \mathrm{N}$).

$$\sum_{j|(i,j)\in A^P} Q_{i,j} - \sum_{j|(j,i)\in A^P} Q_{j,i} = q_i, \forall i \in N \tag{5}$$

Where $\mathrm{q_I}$ indicates the node flow, $\mathrm{q_I}$ is positive when the injection flow enters the pipeline, and negative when the offload flow leaves the pipeline.

The Centrifugal gas compressor is modeled by the compressor characteristic map. The characteristic curve under each rotational speed refers to the relationship between the pressure ratio, polynomial efficiency, power, and flow rate. In particular, the flow rate is

estimated under the compressor entrance condition (the inlet pressure and the inlet temperature). The mutual conversion relations of custody fallow rate and inlet flow rate are shown as follows.

$$Q'_{i,j} = \frac{p_0}{p_i}\frac{T_i}{T_0}Z_{i,j}Q_{i,j}, \forall(i,j) \in A^C \quad (6)$$

Where, $\mathrm{Q'_{I,j}}$ is the flow rate between node i and node j under the compressor inlet condition, $\mathrm{p_0}$ is the custody transfer pressure ($1.01325 \times 10^5 Pa$), $\mathrm{T_0}$ is the custody transfer temperature ($293.15K$), $\mathrm{T_I}$ is the inlet temperature. The equation applies to any compressor arc ($\forall(\mathrm{I,j}) \in \mathrm{A^C}$).

The affinity laws for turbo-machines (sometimes also called the fan laws) applies to centrifugal compressor based on the homologous theory[7]. The simplified representation of the compressor map may be obtained based on the equation shown as follow.

$$\frac{h_{i,j}}{\omega_{i,j}^2} = b_1 + b_2\frac{Q'_{i,j}}{\omega_{i,j}} + b_3\left(\frac{Q'_{i,j}}{\omega_{i,j}}\right)^2, \forall(i,j) \in A^C \quad (7)$$

$$e_{i,j} = b_4 + b_5\frac{Q'_{i,j}}{\omega_{i,j}} + b_6\left(\frac{Q'_{i,j}}{\omega_{i,j}}\right)^2, \forall(i,j) \in A^C \quad (8)$$

Where h indicates the adiabatic compression head (m), ω is the compressor rotational speed (rpm), Q is the flow rate under inlet conditions, and e is the compression efficiency. $\mathrm{b_1, b_2, b_3, b_4, b_5, b_6}$ are the quadratic polynomial coefficient.

$$h_{i,j} \le S_1 + S_2Q'_{i,j} + S_3{Q'_{i,j}}^2, \forall(i,j) \in A^C \quad (9)$$

$$h_{i,j} \ge C_1 + C_2Q'_{i,j} + C_3{Q'_{i,j}}^2, \forall(i,j) \in A^C \quad (10)$$

When the inlet flow decreases to a certain value, the centrifugal compressor cannot work stably, the flow occurs pulsation phenomenon and vibration intensifies. This unstable working condition is called "surge condition", so the left end of the compressor characteristic is restricted by Equ.9. What is more, the pressure ratio and efficiency drop vertically when the flow rate exceeds a certain value which is known as the chock phenomenon. And the right end of the compressor characteristic is restricted by Equ.10. Where, $\mathrm{S_1, S_2, S_3, C_1, C_2, C_3}$ are the polynomial coefficient and the equation applies to any compressor arc ($\forall(\mathrm{I,j}) \in \mathrm{A^C}$).

The compression process in a centrifugal compressor can be well formulated using the isentropic process based on the fact that the flow speed of gas in the compressor is so fast that there is no time to exchange heat with the environment. The relationship between the adiabatic compression head and the pressure ratio is expressed by the following equation.

$$\frac{h_{i,j}g}{1000} = \frac{Z_{i,j}RT}{M_{i,j}}\frac{k}{k-1}\left[\left(\frac{p_j}{p_i}\right)^{\frac{k-1}{k}} - 1\right], \forall(i,j) \in A^C \quad (11)$$

Where, $\mathrm{M_{I,j}}$ is the average molecular mass of the gas (g/mol). In terms of the pipeline network with multiple injection sources, the molecular mass varies with the pipeline section. k is the average isentropic exponent of the gas.

For a certain hydrogen blending ratio, there are many operation control modes in the pipe network to achieve that ratio (different rotational speed control or differential pressure control). However, we want to control the pipeline to operate at the lowest power consumption point. The equation for compressor power calculation can be expressed as follows:

$$N_{i,j} = \frac{Q_{i,j}\rho_{i,j}h_{i,j}g}{1000 \cdot e_{i,j}}, \forall(i,j) \in A^C \quad (12)$$

Where, $\mathrm{\rho_{I,j}}$ is the mixed gas density between node i and node j($\frac{kg}{m^3}$). In terms of the pipeline network with multiple injection sources, the gas density varies with the pipeline section. g is the gravitational acceleration factor. The equation applies to any compressor arc ($\forall(\mathrm{I,j}) \in \mathrm{A^C}$).

$$\omega_{min} \le \omega_{i,j} \le \omega_{max} \quad (13)$$

$$p_{min} \le p_i \le p_{max} \quad (14)$$

$$\varepsilon_{min} \le \varepsilon_{i,j} \le \varepsilon_{max} \quad (15)$$

The rotational speed ω of all compressors, the pressure $\mathrm{p_I}$ of all nodes, and the pressure ratio $\mathrm{\varepsilon_{I,j}}$ of all compressors are comprised of lower and upper bounds as represented.

2.3 Economic and environmental evaluation

The natural gas compressor is driven by the gas turbine generally, so the economic evaluation of the natural gas pipeline network can be determined by the gas consumption and the gas price as shown in Equ.16. Equ.17 formulated the mixed gas calorific value, and Equ.18 formulated the natural gas price.

$$Ec = \left(\sum_{(i,j)\in A^C} N_{i,j}\right)\frac{C}{e_m e_d HV} \quad (16)$$

$$HV = HV_{H_2} \cdot \theta + HV_{NG}(1-\theta) \quad (17)$$

$$C = C_e\frac{HV}{HV_{NG}} \quad (18)$$

The required power of the gas turbine is equal to the summation of the compressor power divided by mechanical efficiency e_m and driver efficiency e_d. HV denotes the lower heating value of the mixed gas (MJ/m^3) and it is related to the value of natural gas,

hydrogen, and the blending ratio. C denotes the natural gas price ($\$/m^3$). The higher the heat value, the higher the gas price. So, the mixed gas price is determined by the heat value of the mixed gas and the pure natural gas, and c_e is the price indicator that represents the basic price for a stander cubic meter of gas ($\$/m^3$). Therefore, the economic cost of the system is $(\sum_{(i,j)\in A^C} N_{i,j})\frac{c_e}{HV_{NG}}$ which is independent of the hydro-blending ratio.

$$Em = (\sum_{(i,j)\in A^C} N_{i,j})\frac{EF}{e_m e_d HV} \quad (19)$$

$$EF = EF_{ng}(1-\theta) \quad (20)$$

Equ.19 and Equ.20 formulate the carbon emission of the system. Carbon emission comes from natural gas combustion, so the total emission is equal to the consumed gas product the carbon emission factor EF ($kg\ CO_2/m^3$). The EF of the mixed gas is determined by the emission factor of natural gas (EFNG) and blending ratio because no carbon is released when burning hydrogen.

3. CASE STUDY

A gun barrel natural gas pipeline with a single gas source and single offload station is studied. The gun barrel pipeline case is used to demonstrate the optimal operation plan under different hydrogen blending ratios and estimate the influence of hydrogen on the operation parameters under different boundary conditions. We propose four scenarios to show the difference in the allowable blending ratio in various situations and the reason that limits further blending is analyzed. The pipeline topology is shown in Fig 1. The orange node indicates the gas source while the blue node represents the offload station. The fundamental parameters of all the arcs (pipeline and compressor) are shown in table 1. The quadratic fitting parameters of the compressor characteristic curve (Equ.7-10) are shown in table 2.

Table 1. The fundamental parameters of all the arcs

Arc type	From node	To node	Length (km)	Diameter (mm)
Pipeline	1	2	100	406
Pipeline	3	4	30	406
Compressor	2	3	-	-

Table2. Quadratic parameters in the constraints

	Constant term	Linear factor	Quadratic factor
Equ.7	-3.42×10^{-4}	1.23×10^{-3}	-4.62×10^{-4}
Equ.8	5.97×10^{-2}	0.849	-0.240
Equ.9	-7.30×10^{4}	22.5	-1.35×10^{-3}
Equ.10	4.36×10^{4}	-11.2	7.28×10^{-4}

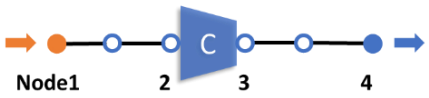

Fig. 1 Topological structure of the cases

Scenario setting: Different control modes are applicable in the operation of the natural gas pipeline network. In summary, the three most commonly used methods are flow rate control, node pressure control, and heat flow rate control, respectively. Therefore, four scenarios are set in this paper, namely, the baseline scenario (BS), the setpoint of flow rate scenario (SF), the setpoint of pressure scenario (SP), and the setpoint of the heat flow rate scenario (SH). In BS, the pipeline network transports pure natural gas with no hydrogen blended where the flow rate control method is chosen. Based on this operation point, the other three scenarios transport the gas with hydrogen blended under the constraints of the hydraulic and the corresponding control mode. The boundary restrictions of variables in different scenarios are shown in table 3. Take the pressure of node 4 as an example. In BS, SF or SH, the pressure should be greater than 40 bar (Lower bound) and lesser than 120 bar (Upper bound), while in SP, the lower bound equal to the upper bound means the pressure of node 4 is set to a constant value of 40 bar. The other variables take the same logic.

Table 3. The boundary of variables in different scenarios

	Unit	Applicable Scenario	Lower bound	Upper bound
Node1 pressure	bar	BS, SF, SH, SP	110	110
Node2 pressure	bar	BS, SF, SH, SP	40	120
Node3 pressure	bar	BS, SF, SH, SP	40	120
Node4 pressure	bar	BS, SF, SH	40	120
Node4 pressure	bar	SP	40	40
Rotational speed	rpm	BS, SF, SH, SP	4000	6000
Pressure ratio	-	BS, SF, SH, SP	1.2	1.8
Offtake flow rate	$10^6m^3/d$	BS, SF	9	9
Offtake flow rate	$10^6m^3/d$	SH, SP	0	Infinity
Offtake heat flow rate	GJ/h	SH	12750	12750
Offtake heat flow rate	GJ/h	BS, SF, SP	0	Infinity

Taking the characteristic map as the carrier, the operating point of the compressor in different scenarios and the changing process from the baseline scenario to other scenarios are shown in Fig.3. Firstly, the operating parameters of the system in BS are analyzed. Then, the other three scenarios are analyzed in turn and compared with the benchmark respectively.

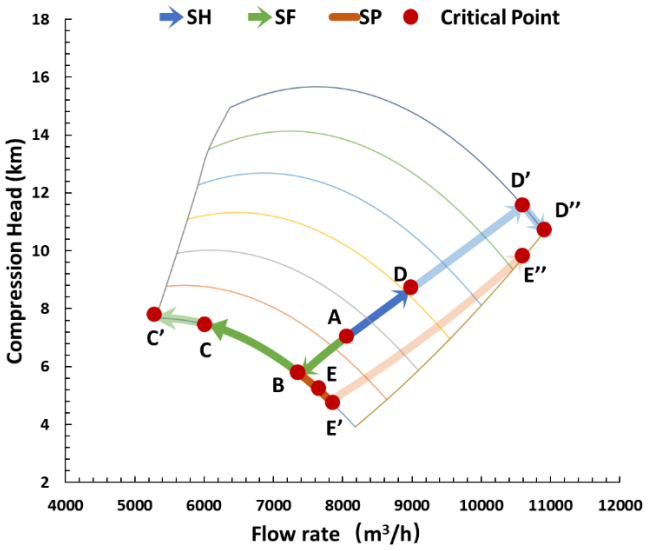

Fig.3. the operating point and the changing process during different scenarios

In the baseline scenario, the standard flow rate is set to nine million cubic meters per day and other boundary settings can be seen in table 3. In BS, the hydrogen blending ratio is zero, so the density, molar mass, and other characteristics of pipeline gas are equal to those of purely natural gas. We proposed an operation optimization model with the minimum energy consumption of the compressor as the objective function (see Equ.3), and the best operating point (called the BECP: best energy consumption point) in BS is obtained (see point A in Fig.3).

The physical properties of the mixed gas, the operating parameters of the compressor, and the node pressure can be seen in table 4. Performing the optimization scheme, the compression head is 7236 meters following the inlet flow rate of 8181 cubic meters per hour. The transmission power before the optimization is 6322 kW, 11.48% higher than that in the new plan. The result of optimization can be seen in this view: the compressor provides the smallest energy head so the endpoint pressure equals its minimum value of 40 bar.

Table 4. Variables value in different scenarios

		Unit	Point A	Point B	Point C	Point D	Point E
Mixed gas	Blending ratio	%	0	7.91	27.3	2.52	19.39
	Density	kg/m^3	0.62	0.58	0.47	0.61	0.52
	Molecular weight	g/mol	16.04	14.93	12.21	15.69	13.32
	Flow rate	10^6m^3/d	9	9	9	9.16	9.27
Node pressure	Node1	bar	110	110	110	110	110
	Node2	bar	42.76	48.4	60.33	40	49.64
	Node3	bar	69.08	69.36	86.76	69.5	67.28
	Node4	bar	40	40	70.62	40	40
Compressor	Inlet flow rate	m^3/h	8181.96	7385.12	6071.85	8973.16	7461.20
	Efficiency	-	0.81	0.80	0.76	0.81	0.8
	Compression head	m	7236.72	5728.92	7422.83	8648.69	5590.84
	Power	kW	5671.71		4533.88	6746.02	3759.58
	Pressure ratio	-	1.62	1.42	1.44	1.74	1.36
	Rotational speed	rpm	4460	4000	4000	4884	4000

In SF scenario, the maximum hydrogen blending ratio is 27.31% (point C). At this time, the density and molar mass of the mixed gas is 0.47 kg/ m^3 and 12.21 g/mol respectively. Taking the characteristic curve of the compressor as the carrier, in pace with the blending ratio increasing from 0 to 27.31%, the change line of the operation point of the compressor is shown as the green line in Fig.3. In SF, the pressure of node 1 is constant at 110 bar while the density of the mixed gas gradually decreases with hydrogen blending. According to Equ.4, the pressure drops required to transport gas with the same flow rate decrease. Therefore, the inlet pressure of the compressor (node 2) increases, and the inlet flow rate decreases as Fig.3 shows.

The variation of the operation point is divided into two stages, where the compressor speed gradually

decreases in the first stage (point A to point B) and the point moves to the left along the characteristic curve at the lowest speed in the second stage (point B to point C). In the first stage, the compressor speed and the compression head decrease as the inlet flow decreases. Although the compressor provides less energy, due to the pressure drops required to transport fixed flow rate decrease, it can still ensure that the terminal pressure of the pipeline is exactly equal to the minimum allowable pressure (node 4 pressure is kept constant in the first stage). In the second stage, the speed has dropped to the lowest value, the operating point will move to the left along the characteristic curve at the lowest speed as the hydrogen doping ratio continues to increase. At this time, the compression head gradually increases, and the terminal pressure will be greater than the minimum value. The surge and chock flow rates at the lowest speed are 5303 and 8181 m^3/h. To keep the operating point within the middle 50% range, the maximum hydrogen blending ratio is set to 27.31% (point C) with a minimal inlet flow rate.

The node pressure and the compressor parameters of operating point C can be seen in table 4. Compared to the BS, the compressor power of point C is reduced from 5671kW to 4533kW, a 20.07% decrease; the compressor power of point B is reduced from 5671kW to 4533kW, a 26.27% decrease. In conclusion, the compressor power and operation cost decrease with the increase of hydrogen doping ratio in SF, but the contrary trend occurs when the compressor speed reaches the lower limit. Compare point C to point A, the annual operation cost is reduced from 22.23 million dollars to 17.77 million dollars, a 20.07% decrease (the same as the compressor power), and the annual carbon emission is reduced from 10.63 kilotons to 7.57 kilotons, a 28.73% decrease.

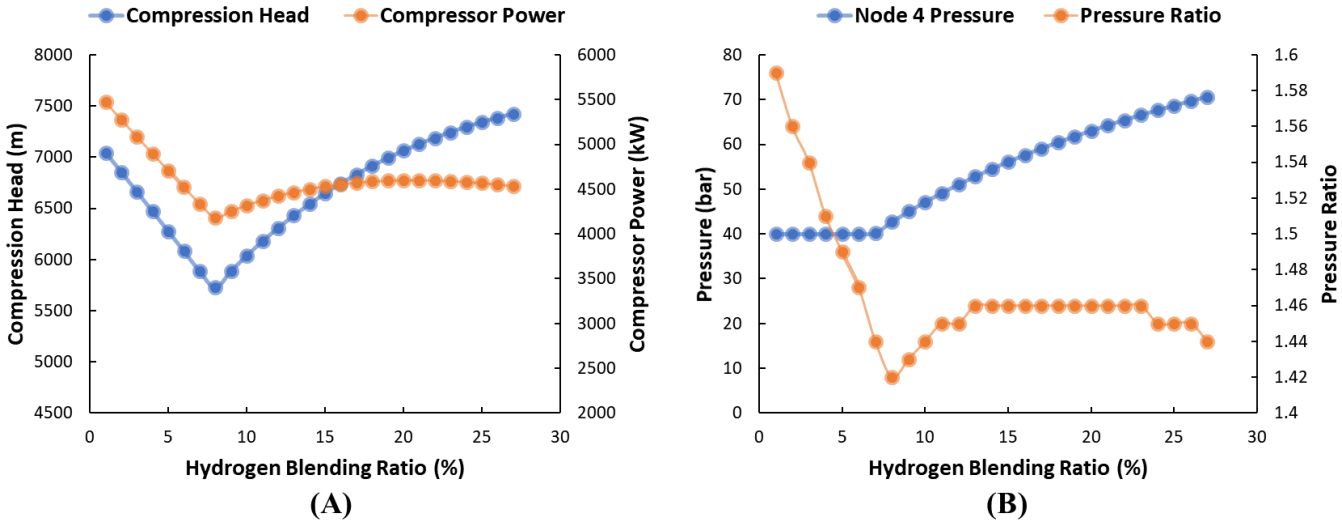

Fig.4. Changes of the operating parameters in SF

In the SH scenario, the maximum hydrogen blending ratio is 2.52%. With the blending ratio increasing from 0 to 2.52%, the change line of the operating point of the compressor is shown as the blue line in Fig.3.

The lower heating value of hydrogen is $11\mathrm{MJ}/\mathrm{m}^3$ while natural gas takes a value of about $34\mathrm{MJ}/\mathrm{m}^3$. As the case in SH illustrated, in general, the heat flow rate of hydrogen-mixed gas transported by the same pressure drop is smaller than that of purely natural gas. On the premise of constant heat flow and start point pressure, the inlet pressure of the compressor (node 2) decreases, and the corresponding inlet flow increases. In this process, the rotational speed of the compressor creeps up from point A to point D as Fig.3 shows. Note that the terminal pressure keeps the minimum allowed value to save the energy consumption of the. Although the density of the mixed gas decreases, the power shows an upward trend due to the increase in compression head and standard flow rate compressor.

In this scenario, the maximum blending ratio is relatively small. That is because the pressure of node 2 is 42.76 bar in BS, which is only 2.76 bar higher than the lower pressure boundary. In the hydrogen blending process, the pressure of node 2 gradually decreases to the lower limit of 40 bar. The margin for its decline is small, and so do the corresponding maximum blending ratio.

The parameters of operating point D can be seen in table 4. Compared to the BS, the compressor power of point D increased from 5671kW to 6746kW, an 18.96% increase. In SH, the factor that constrains further hydrogen blending is the lower boundary of the node pressure. If the lower boundary of the node pressure is reduced, the operation point will move along with the

tendency line of AD continuously (point D to D'). When the compressor speed reaches the upper limit, the point will move to the right along the corresponding characteristic curve (point D' to D''). The variation trend of operation points in SF and SH is completely opposite. The annual operation cost is increased from 22.23 million dollars to 26.44 million dollars, an 18.96% rise (the same as the compressor power), and the annual carbon emission is increased from 10.63 kilotons to 12.53 kiloton, a 17.97% increase.

In the SP scenario, the maximum hydrogen blending ratio is 19.39%. With the blending ratio increasing from 0 to 19.39 %, the change line of the operating point of the compressor is shown as the orange line in Fig.3.

Keeping the starting and ending pressure of the pipe network the same as that in BS (see operation point A in Fig.3), the optimal operating point following a step change from point A to point B. The standard flow rate in operating point B is 8.85×106 m^3/d, 1.67% lower than 9 ×106 m^3/d in point A, and the compressor power is 4439kW, a 21.72% lower than 5671kW in point A. The step change result demonstrated that the system reduces the throughput flow rate under the premise of keeping the endpoint pressure unchanged to achieve BECP.

In pace with the increase of the hydrogen blending ratio, the operating point move to the right along the characteristic curve at the lowest speed. To keep the operating point within the middle 50% range, the maximum hydrogen blending ratio is set to 19.39% (point E) with the maximum inlet flow rate. The stander flow rate gradually increases from 8.85×10^6 m^3/d to 9.26× 10^6 m^3/d with a 4.6% increase. Although the flow rate increases, the density decreases to a large extent, so node 2 pressure (i.e. the inlet of the compressor) shows an increasing trend. Similarly, to make full use of the pressure at the endpoint, the node 4 pressure remains unchanged at 40 bar, so the outlet pressure of the compressor decreases gradually. Accordingly, the pressure ratio and power of the compressor are gradually reduced. The energy consumption of the whole system reaches the lowest value of 3759 kW until the operating point reaches point E.

If the upper boundary of the compressor inlet flow rate is increased, the operation point will move along with the tendency line of BE continuously. During the process, the pressure ratio of the compressor gradually decreases until it reaches the lower limit of 1.2 at the operating point E'. Then, it is impossible to increase the pressure of node 2 and reduce the pressure of node 3 continuously. However, the flow rate of the system still increases gradually in the wake of the hydrogen blending. To meet the transportation requirements, the optimal operating point keeps the pressure ratio constant at 1.2, and the speed of the compressor is gradually increased from 4000 rpm to 5692 rpm to deliver more gas. When the operating point reaches point E'', the inlet flow rate is so large that the compressor is working in the choking condition.

The annual operation cost is reduced from 22.23 million dollars to 14.73 million dollars, a 33.71% decrease (the same as the compressor power), and the annual carbon emission is reduced from 10.63 kilotons to 6.53 kiloton, a 38.50% decrease.

4. CONCLUSIONS AND FUTURE DIRECTIONS

Hydrogen injection in the natural gas pipeline has a certain influence on the operating conditions of the pipeline network and the compressors. Both the operation cost and the carbon emission will decrease when the pipeline system is optimized. The annual economic cost of the original plan is 24.78 million dollars and the carbon emission is 11.84 kilotons. This paper optimized the operation plan by adjusting the speed of the compressor. Then, the economic cost is reduced from 24.78 to 22.23 million dollars with an 11.48% decline, and the carbon emission is reduced from 11.84 to 10.63 kilotons also with an 11.48% decline. Moreover, optimization makes the natural gas pipeline adapt to more hydrogen blending compared with other plans such as fixing the compressor speed.

The operating parameters will change along with the hydrogen blending amount and the boundary control model. In SF: the operation cost and the carbon emission decrease with the increase of the hydrogen doping ratio, but the contrary trend occurs when the compressor speed reaches the lower limit. The operation cost and the carbon emission have a 20.07% and 28.73% reduction when the hydrogen blending rate is 27.3% in SF. In SH, the variation trend of operation points and the economic and environmental performance in opposite from that in SF. The operation cost and the carbon emission have an 18.96% and 17.97% increase when the hydrogen blending rate is 2.52% in SF. In SP, the operation cost and the carbon emission decrease with the increase of the hydrogen doping ratio. The operation cost and the carbon emission have a 33.71% and 38.50% reduction when the hydrogen blending rate is 19.39 % in SF. When the costs decrease after hydrogen doping, the carbon emission will take more reduction. Conversely, the carbon emission will take less increase when the costs rise after hydrogen doping.

The maximum hydrogen blending ratio varies a lot in different scenarios (27.3% in SF, 2.52% in SH, and 19.39%

in SP). The factors that restrict further blending are different. For the centrifugal compressor map, the factors may include surge line, chock line, and maximum or minimum rotational speed. For the upper or the lower boundaries of the variables, the factors may include pressure, flow rate, gas velocity or pressure ratio, etc. This result can help the decision-maker determine whether it is necessary to replace (improve) some equipment in the pipe network system or adjust some boundary restrictions to adapt to more hydrogen blending.

Future directions: For future studies, the following directions are recommended. Firstly, accurate and fast algorithms are needed for large-scale pipe networks. A single optimization problem requires solving a nonconvex mixed-integer nonlinear program, which means getting the variation laws of operating parameters through the discretization method may be time-consuming or even impracticable. So, fast algorithms are needed to reduce single calculation time. Secondly, this paper is exclusively focused on the operating characteristics of the natural gas pipeline and compressor after hydrogen blending from the perspective of hydraulics. Furthermore, the comprehensive model that considered material safety, leakage, and downstream extraction as constraints can be extended in future studies.

ACKNOWLEDGEMENT

This work was part of the Program “Study on Optimization and Supply-side Reliability of Oil Product Supply Chain Logistics System” funded under the National Natural Science Foundation of China, grant number 51874325. The authors are grateful to all study participants.

REFERENCE

[1] H. Council. (2017). Hydrogen scaling up: A sustainable pathway for the global energy transition. Available: https://hydrogencouncil.com/wp-content/uploads/2017/11/Hydrogen-Scaling-up_Hydrogen-Council_2017.compressed.pdf

[2] R. R. Ratnakar et al., "Hydrogen supply chain and challenges in large-scale LH2 storage and transportation," International Journal of Hydrogen Energy, vol. 46, no. 47, pp. 24149-24168, 2021/07/09/ 2021.

[3] I. Eames, M. Austin, and A. Wojcik, "Injection of gaseous hydrogen into a natural gas pipeline," International Journal of Hydrogen Energy, vol. 47, no. 61, pp. 25745-25754, 2022/07/19/ 2022.

[4] W. Keith and W. Heikkila, "2 - Kirchhoff's laws," in Earth's Magnetosphere (Second Edition), W. Keith and W. Heikkila, Eds.: Academic Press, 2021, pp. 89-117.

[5] G. S. Soave, "An effective modification of the Benedict–Webb–Rubin equation of state," Fluid Phase Equilibria, vol. 164, no. 2, pp. 157-172, 1999/10/28/ 1999.

[6] R. Hernández-Gómez, D. Tuma, D. Lozano-Martín, and C. R. Chamorro, "Accurate experimental (p, ρ, T) data of natural gas mixtures for the assessment of reference equations of state when dealing with hydrogen-enriched natural gas," International Journal of Hydrogen Energy, vol. 43, no. 49, pp. 21983-21998, 2018/12/06/ 2018.

[7] E. Shashi Menon, "Chapter Ten - Compressor Stations," in Transmission Pipeline Calculations and Simulations Manual, E. Shashi Menon, Ed. Boston: Gulf Professional Publishing, 2015, pp. 369-404.